THE JOURNAL OF BIOLOGICAL CHEMISTRY
Vol. 277, No. 50, Issue of December 13, pp. 48677–48684, 2002
Printed in U.S.A.

Characterization of the Apoptosis Suppressor Protein P49 from the *Spodoptera littoralis* Nucleopolyhedrovirus*

Received for publication, August 28, 2002, and in revised form, September 24, 2002
Published, JBC Papers in Press, September 24, 2002, DOI 10.1074/jbc.M208810200

Zifei Pei‡§¶, Galit Reske‡¶, Qihong Huang, Bruce D. Hammock‖, Yipeng Qi§, and Nor Chejanovsky‡ ‡‡**

From the ‡Entomology Department, Institute of Plant Protection, Agricultural Research Organization, the Volcani Center, POB 6, Bet Dagan, 50250 Israel, the §Institute of Virology, Wuhan University, Wuhan 430072, People's Republic of China, and ‖Department of Entomology, University of California, Davis, California 95616

Two antiapoptotic types of genes, *iap* and *p35*, were found in baculoviruses. P35 is a 35-kDa protein that can suppress apoptosis induced by virus infection or by diverse stimuli in vertebrates or invertebrates. *iap* homologues were identified in insects and mammals. Recently, we have identified *sl-p49*, a novel apoptosis suppressor gene and the first homologue of *p35*, in the genome of the *Spodoptera littoralis* nucleopolyhedrovirus. Here we show that *sl-p49* encodes a 49-kDa protein, confirmed its primary structure that displays 48.8% identity to P35, and performed computer-assisted modeling of P49 based on the structure of P35. We demonstrated that P49 is able to inhibit insect and human effector caspases, which requires P49 cleavage at Asp^{94}. Finally we identified domains important for P49's antiapoptotic function that include a reactive site loop (RSL) protruding from a β-barrel domain. RSL begins at an amphipathic α1 helix, traverses the β-sheet central region, exposing Asp^{94} at the apex, and rejoins the β-barrel. Our model predicted seven α-helical motifs, three of them unique to P49. α-Helical motifs α_1, α_2, and $\alpha_{4'}$ were required for P49 function. The high structural homology between P49 and P35 suggests that these molecules bear a scaffold common to baculovirus "apoptotic suppressor" proteins. P49 may serve as a novel tool to analyze the contribution of different components of the caspase chain in the apoptotic response in organisms not related phylogenetically.

Apoptosis is a normal physiological cell suicide program highly conserved among vertebrates and invertebrates (1–4). This cell death program plays a critical role during normal development, tissue homeostasis, eliminating from the organism unwanted cells, including damaged and virus-infected cells. Thus, animal viruses have evolved ways to evade, delay, or suppress this important cell defense strategy (for a review, see Ref. 5).

Baculoviruses possess two types of genes with antiapoptotic activity, *iap* (inhibitor of apoptosis) and *p35*, that can suppress apoptosis induced by virus infection or by diverse stimuli in vertebrates or invertebrates (6–9). Cellular homologues of *iap* genes were identified in the genomes of insects and mammals (10–12). P35, a 35-kDa protein encoded by the *p35* gene of the *Autographa californica* multiple nucleopolyhedrovirus (AcMNPV),[1] inhibits a broad range of caspases, including human and insect caspases (13–17), activated during programmed cell death (reviewed in Ref. 18). The crystal structure of P35 was determined (19), providing insight into the mechanism of caspase inhibition (20). The most remarkable feature of P35's structure is the presence of a large loop domain (residues 60–98), called reactive site loop (RSL), protruding above a central β-sheet core. The RSL is exposed to the solvent and contains at its apex the caspase cleavage site Asp^{87} ↓ Gly^{88} in the caspase recognition motif ^{84}DQMD^{87} (19, 20). The RSL is maintained and stabilized by a single amphipathic α_1-helix that traverses and interacts with the top of the β-sheet core (19). Recently, we have identified *sl-p49* (previously designated *slp49*), a functional apoptosis suppressor gene and the first homologue of the *p35* gene, in the genome of the *Spodoptera littoralis* nucleopolyhedrovirus (21). *Sl-p49* encodes a predicted 49-kDa protein that showed 48.8% identity to P35. We took advantage of the high degree of similarity of the putative P49 molecule to P35 and modeled P49 utilizing the P35 structure as the template of reference. In this study, we report for the first time the expression, identification, and functional activity of P49. We demonstrate that P49 is able to inhibit insect and human effector caspases that require cleavage at Asp^{94} for function and characterize domains important for the antiapoptotic function of P49.

EXPERIMENTAL PROCEDURES

Cell Lines and Viruses—Spodoptera frugiperda SF9, *Bombyx mori* BmN, and *Trichoplusia ni* TN368 (22) cells were maintained and propagated in TNM-FH medium supplemented with 10% heat-inactivated fetal bovine serum (23). Wild type AcMNPV E-2 strain, *S. littoralis* nucleopolyhedrovirus E-15 strain, and recombinant AcMNPV viruses and vΔP35K/pol+ were described previously (16, 21, 23).

Marker Rescue Assay and Isolation of Recombinant Viruses—The ability of an antiapoptotic gene to enable replication of P35-defective AcMNPV viruses, inhibiting apoptosis of SF9 cells, was monitored by microscopic observation of the presence of viral polyhedra in the nuclei

* This work was supported by Israel Science Foundation Grant 426/99-3 and in part by Fogarty International Research Collaboration Award Grant TW01219, and United States Department of Agriculture Grant 35302-09919 (to B. D. H.) contribution from the Agricultural Research Organization (The Volcani Center, Bet Dagan, Israel) No. 415/02. The costs of publication of this article were defrayed in part by the payment of page charges. This article must therefore be hereby marked "*advertisement*" in accordance with 18 U.S.C. Section 1734 solely to indicate this fact.

The nucleotide sequence(s) reported in this paper has been submitted to the GenBank™/EBI Data Bank with accession number(s) AF448494.

¶ These two authors contributed equally to this work.

** Present address: The Scripps Research Institute, 10550 N. Torrey Pines Rd., La Jolla, CA 92307.

‡‡ To whom correspondence should be addressed: Entomology Dept., Institute of Plant Protection, Agricultural Research Organization, The Volcani Center, POB 6, Bet Dagan, 50250 Israel. Tel.: 972-3-9683694; Fax: 972-3-9604180; E-mail: ninar@volcani.agri.gov.il.

[1] The abbreviations used are: AcMNPV, *A. californica* multiple nucleopolyhedrovirus; RSL, reactive site loop; CHAPS, 3-[(3-cholamidopropyl)dimethylammonio)]-1-propanesulfonic acid; DTT, dithiothreitol; DEVD, Asp-Glu-Val-Asp-CHO.

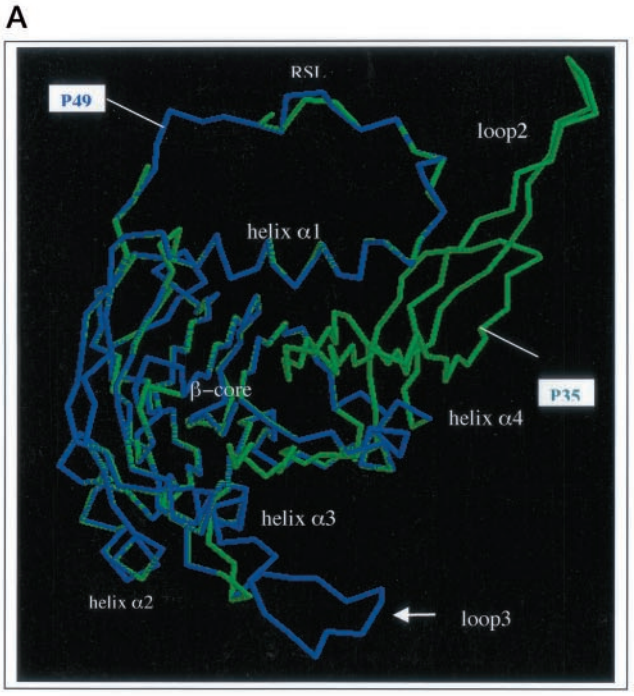

FIG. 1. *A*, P49 model. Three-dimensional superimposition of P49 (blue chain amino acids 1–236) on the resolved crystal structure of P35 (*green chain*, amino acids 1–299; Protein Data Bank code 1P35) (20). Main structural elements are indicated. *B*, P49-P35 alignment. *Horizontal dots* indicate gaps made to optimize the alignment; *vertical bars* and *dots*, identical and similar amino acids, respectively. The major secondary structural elements are indicated in *italic type above* and *below* each polypeptide sequence. *h*, helix and α-respective number; *s*, strand. Identified loops are *underlined*. *L3*, side loop 3; *L2*, C-terminal loop 2.

of infected cells (7, 8, 21). Routinely, 1 μg of vΔP35K/pol+ DNA and 1 μg of tested plasmid DNA were co-transfected into 4×10^5 SF9 cells using Lipofectin (Invitrogen) in triplicates. 3–4 days after transfection, the cells were examined by light microscopy for the presence of polyhedra. The rescued virus yields were evaluated by titration in SF9 cells and counting the number of nonapoptotic polyhedra-positive plaques (16, 21).

Cloning of B. mori Caspase-1—mRNA was isolated from BmN cells by using an mRNA extraction kit (Qiagen). Degenerate primers were designed according to the consensus amino acid sequence among the members of the insect caspase family, 5′-CA(A/G)GC(A/C/G/T)TG(T/C)C A(A/G)GG(A/C/G/T)GA-3′ and 5′-TGCAT(A/G)(A/T)ACCA(A/C/G/T)GA(A/C/G/T)CC-3′. Reverse PCR was performed to obtain full-length *B. mori* caspase-1 cDNA, and 5′-RACE and 3′-RACE were performed from BmN mRNA by using a 5′-RACE system (Invitrogen) and 3′-RACE kit (Takara), respectively. PCR primer 5′-AGAGTAATAACCTGGTACCGT-3′ and a kit primer were used in the 5′-RACE PCR, and the primer 5′-TGGAGAAACACAACTCGTG-3′ and a kit primer were used in the 3′-RACE PCR. All amplified fragments were cloned into *Hin*cII site of pTZ19U and sequenced.

Caspase Assays—For caspase inhibition assays, serial dilutions of wild type or mutated P49-His_6 in assay buffer 50 mM HEPES (pH 7.4), 50 mM NaCl, 0.1% CHAPS, 10% sucrose, and 10 mM DTT were mixed with equal volumes of caspase-containing assay buffer (purified *B. mori* caspase-His_6 (25 pmol) or active recombinant human caspase-3 hCPP32 (0.3 pmol, 2 units; Biomol, Inc.), preactivated for 15 min with 10 mM DTT. Ac-DEVD-*p*-nitroanilide (200 μM) was added, and the reaction was monitored colorimetrically at 405 nm using an enzyme-linked immunosorbent assay reader (Tecan GmbH). Values, reported as the rate of product formation, correspond to the average of triplicate assays taken during linear product release within the first 10% of each reaction.

S. frugiperda Apoptotic Extracts—SF9 cells were collected at various time points after vAcΔp35/pol+ infection and suspended in a solution of 10 mM HEPES (pH 7.0), 0.1% CHAPS, 5 mM DTT, and 2 mM EDTA containing the protease inhibitor mixture E-64 (100 μM), leupeptin (100 μM), pepstatin A (1 μM), aprotinin (2 μg/ml), and phenylmethylsulfonyl fluoride (1 μM) (Calbiochem). After one freeze-thaw cycle, the cells were subjected to Dounce homogenization. The cells lysates were clarified by centrifugation and stored at −80 °C.

Protein Expression and Purification—B. mori caspase-1 was cloned into *Nde*I and *Xho*I sites of PET23b (Novagen) to generate the plasmid pBm-caspase-1 with a C-terminal His_6 tag. *p35* was amplified from the plasmid $pIE1^{hr}$-p35 (24) by PCR using the primers 5′-GGAATTCCATATGTGTGTAATTTTTCC-3′ and 5′-CCGCTCGAGTTTAATTGTGTTTAATA-3′ and cloned into *Nde*I and *Xho*I sites of pET22b(+). Sequencing confirmed that the *p35* clone was correct, and its 3′-end was fused with the His tag of pET. The recombinant proteins were expressed in *Escherichia coli* BL21 (DE3) after induction with 1 mM isopropyl-β-D-thiogalactopyranoside. The cells were collected and suspended in ice-cold 20 mM Tris (pH 8.0) and 500 mM NaCl containing the protease inhibitors E-64 (100 μM), phenylmethylsulfonyl fluoride (1 μM), pepstatin A (1 μM), aprotinin (2 μg/ml), and 1 mg/ml lysozyme. After lysis and further clarification, the extracts were mixed with Ni^{2+}-charged resin (Ni^{2+}-nitrilotriacetic acid; Qiagen) in binding buffer (20 mM Tris (pH 8.0), 5 mM imidazole, and 500 mM NaCl). Unbound material was washed with 20 mM imidazole-containing binding buffer. Bound protein was eluted with 250 mM imidazole-containing binding buffer and was >95% pure as judged by Coomassie-stained polyacrylamide gel analysis. Protein concentration was measured using the Bio-Rad protein assay kit. *B. mori* caspase-1 active concentrations were determined by titration with DEVD-CHO as described before (25).

P49 Expression—sl-p49 was amplified from the plasmid pKS2 (21) by PCR using the primers 5′-CCGGAATTCATGTGTGTACTGATACCAAC-3′ and 5′-ATAGTTTAGCGGCCGCTATATCTATGTAAATGTTACG-3′ and subcloned in Bluescript (Stratagene). The obtained plasmid pBlue-49 was subsequently digested with *Eco*RI and *Not*I and subcloned into pET22b(+), to provide it with a C-terminal His_6 tag. The resultant plasmid was digested with *Bpu*1102I, and the cohesive end

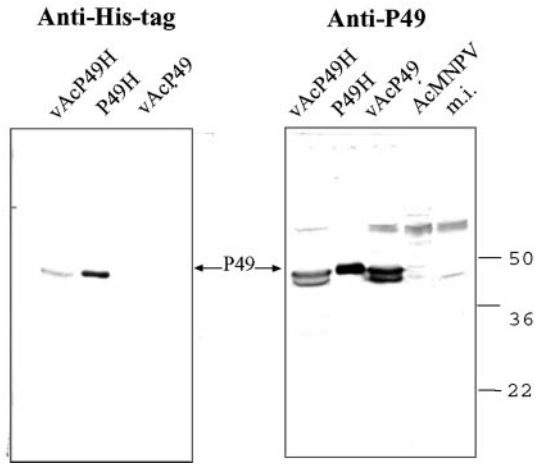

FIG. 2. **Overexpression of P49 and His-tagged P49 using baculovirus vectors.** SF9 cells were infected with vAcP49 or vAcP49H at a multiplicity of infection of 25. Protein extracts were prepared at 72 h postinfection and subjected to affinity chromatography using Ni^{2+}-conjugated agarose beads. The crude extracts and purified P49 were subjected to SDS-PAGE followed by immunoblot analysis with anti-His tag or anti-P49 antiserum (*left* and *right panel*, respectively). *AcP49H* and *vAcP49*, crude extract from vAcP49H- and vAcP49-infected cells, respectively; *P49H*, purified P49-His-tagged protein; *AcMNPV* and *m.i.*, wild type-infected and mock-infected cell extract, respectively. Molecular markers (in kDa) are indicated on the *right*.

was treated with Klenow. The complete *sl-p49*-His open reading frame was rescued by subsequent digestion with *Eco*RI and subcloning into *Eco*RI- and *Stu*I-digested pFastBacI (Invitrogen) to get p49 FastBac-His and, after it, the corresponding BACmid bacp49H by following the manufacturer's instructions (Invitrogen). bacp49H DNA was transfected to SF9 cells to produce the recombinant baculovirus vAc49H. DNA sequencing confirmed the identity of plasmids and viral constructs. 5×10^6 SF9 cells infected with recombinant baculoviruses (multiplicity of infection of 25) expressing either (*a*) P49 or (*b*) P49H were harvested at 48 h after infection in lysis buffer. After cell disruption by freezing and thawing, the clarified lysates were (*a*) subjected to SDS-PAGE, and the gel was stained with Coomassie Blue (overexpressed P49 was identified by comparing the polypeptides synthesized in extracts from vAcP49- and wild type AcMNPV-infected cells) or (*b*) mixed with Ni^{2+}-conjugated agarose beads (Qiagen) in binding buffer for 2 h at 4 °C. Washing and elution were performed with 30 and 250 mM imidazole, respectively.

Immunoblot Analysis—Proteins were subjected to SDS-PAGE and to immunoblot analysis (26, 27) using either anti-P49 (prepared by injection of P49 into rabbits using standard procedures) or mouse monoclonal anti-His antisera (Invitrogen).

P49 Modeling—Computer-assisted modeling of P49 was based on the recently determined structure of P35 (19), exploiting the availability of the Swiss-Model and 3D-PSSM Web server Biomolecular Modeling Laboratory at the Imperial Cancer Research Fund (28, 29).

IVT P49 Cleavage Assays—The T7 promoter-containing plasmid pBlue-P49-stop was generated by exchanging the C-terminal *Bgl*II-*Sac*I fragment of pBlue-P49 with the homologous fragment from pKS2 (21). Coupled transcription-translation reactions were performed using rabbit reticulocyte lysates and [^{35}S]Met-Cys label (PerkinElmer Life Sciences) as specified by the TNT manufacturer (Promega Corp.). Apoptotic extracts containing *S. frugiperda* protease (16) or activated caspases were incubated for 30 min with or without inhibitors and then mixed with ^{35}S-labeled *in vitro* translated P49. Inhibitors utilized included protease inhibitor mixture (described above), and caspase-II group-specific inhibitor DEVD-CHO (10 μM). All reaction mixtures (20 μl) contained 100 mM HEPES (pH 7.5), 2 mM DTT, 0.1% CHAPS, and 10% sucrose. After a 2-h incubation at 30 °C, the samples were terminated by boiling and subjected to SDS-PAGE in a 15% acrylamide gel followed by fluorography.

P49 Mutagenesis—Mutations in P49 were generated in pBlue-P49-stop by using overlap extension polymerase chain reaction with complementary primers containing the desired mutation (30). The primers utilized were as follows (the mutation sites are underlined, and only one primer of the complementary pair is described for simplicity): C2A, 5′-AACGGCAAAATGGCTGTACTGATACCAACATTC-3′; D28A, 5′-TCGATGCGCGCTCTGATCTATGTG-3′; S55K, 5′-GCGCTAAATATTAAGGGACCCCTCGTGTGCG-3′; R63Q, 5′-CGTGAATAGGGTGTCCATGCACATTGTG-3′; V69K, 5′-CCATGCACATTAAGCACATGTACAGATCG-3′; I76K, 5′-CAGATCGCACAAAGATAGGGTCTTTGATA-3′; I76Y, 5′-ACAGATCGCACTACGATAGGGTC-3′; I76P, 5′-GTACAGATCGCACCCCGATAGGGTCTTTG-3′; F80K, 5′-CGATAGGGTCAAAGATAAATTCAACAAAT-3′; T91A, 5′-ACATATTCGGCGGCCGTGACCGATGGCG-3′; D94A, 5′-CGACCGTGACCGCTGGCGGTGGAGCCGAT-3′; S113A, 5′-TGTCTGCATGGCACGCGGAGATCTTTTAA-3′; L125P, 5′-AATTACAAAAATTGTCCGCTCAACGAAATG-3′; V136P, 5′-TACGACGACCCCGAAAAGTTTAGAAAATAC-3′; Y142A, 5′-GTTTAGAAAAGCCTGTCTCAAACCTTTAA-3′; D159A, 5′-GAGCGGCAGCGCCGTCGGTGTGG-3′; K178A, 5′-GTTGAAACCGGCACTGTTGAATAACAAAAA-3′; I198K, 5′-CGGTCAAGTGAAGGTGCCGCTTATGCAC-3′; I205K, 5′-CTTATGCACGAAAAAACGAAAACGGAAGCG-3′; M218A, 5′-CGTACGAAGTGGCGGCGATGATCAA-3′; L237P, 5′-TGTGCTGGAACGACCGAAGCGTTCCATGG-3′; L376P, 5′-AGTCTTGGAGAACCGTATTCGTTTGTAAA-3′; and K387A, 5′-TTATCGATTGGGCAACACACGAGACCAAT-3′. All mutations were confirmed by DNA sequencing.

TABLE I
Effect of site-directed mutations on P49 antiapoptotic function

Mutation	P49 predicted domain affected	Apoptosis suppression[a]
Wild type	None	+
T91A	RSL	−
D94A	RSL	−
R63Q	Turn	+
V69K	α_1-helix hydrophobic face[b]	−
I76K	α_1-helix hydrophobic face[b]	−
I76Y	α_1-helix hydrophobic face[b]	+
F80K	α_1-helix hydrophobic face[b]	−
C2A	β-sheet	+
D28A	β-sheet	+
S55K	β-sheet	−
I198K	β-sheet	−
S113A	β-sheet	+
M218A	β-sheet[b]	−
D159A	Turn	+
I205K	Turn	+
Y142A	α_3-helix	−
K178A	Turn	+
R236A	α_4-helix	−
R239A	α_4-helix	−
K387A	Turn	+
N-His_6	β-core	−
C-His_6	Solvent?	+
I76P	α_1-helix	−
L125P	α_2-helix	−
L136P	α_3-helix	+
L237P	α_4-helix	−
L376P	α_6-helix	+

[a] The antiapoptotic function of the P49 mutants was determined by measuring their ability to recover the replication of AcΔp35/pol+ after co-transfection with the latter DNA to SF9 cells (see "Experimental Procedures"). Rescued mutants that yielded above 60,000 nonapoptotic polyhedra-positive plaque-forming units/ml recovering the wild type AcMNPV phenotype were considered functional (+), whereas mutations that yielded less than 8000 plaque-forming units/ml were considered not functional (−).

[b] Amino acid residues displayed in detail in Fig. 7*C*.

Determination of P49 Sequence—P49 sequencing was performed at The Protein Research Center (Israel Institute of Technology, Technion, Haifa, Israel). The stained protein band from the SDS-PAGE gel obtained from vAc49-infected Sf9 cell extracts (at 48 h postinfection) was cut with a clean razor blade, and the proteins were reduced with 10 mM DTT and modified with 100 mM iodoacetamide in 10 mM ammonium bicarbonate. The gel piece was treated with 50% acetonitrile in 10 mM ammonium bicarbonate to remove the stain from the proteins, dried, and rehydrated with 10 mM ammonium bicarbonate containing about 0.1 g of trypsin/sample followed by overnight incubation at 37 °C, and the resulting peptides were recovered with 60% acetonitrile with 0.1% trifluoroacetate. The tryptic peptides were resolved by reverse-phase chromatography on a 1 × 150-mm Vydac C-18 column. The peptides were eluted using an 80-min linear gradient of 5–95% acetonitrile with 0.025% trifluoroacetate in water at flow rate of about 40 μl/min. The liquid from the column was electrosprayed into an ion trap mass spectrometer (LCQ; Finnigan, San Jose, CA). Mass spectrometry was per-

A

```
  1 M A D E E K K T N G S G T D Q R K N G N E D E G D G M G Q S W I F T R R R Y A K
 41 M P V E R Y A H Y Y N M N H N N R G M A I I F N H E H F E I H N L K S R T G T N
 81 V D S D S L S K V L R G L G F S V T V L H N L R A E D I N R Y I Q Q I S E M D H
121 T D N D C L L V A V L S H G E L G M L Y A K D T H Y K P D N L W Y Y F T A D K C
161 P T L A G K P K L F F I Q A C Q G D K L D G G I T L S N T E T D G S S S S S Y R
201 I P I H A D F L I V F S T V P G Y Y S W R N T T R G S W F M Q S L C E E L R N Y
241 G T Q R D I L T L L T F V C Q R V A L D F E S N T P D I T P M H Q Q K Q V P C I
281 N S M L T R L L L F G K K *
```

B

```
Bm      15 QRKNGNEDEGDGMGQSWIFTRRRYAKMPVERYAHYYNMNHNNRGMAIIFNHEHFEIHNLK  74
           QR NG  DEGD +G +      R A+MPV+R A YYNMNH +RGMAIIFNHEHF+IH+LK
Sf      18 QRTNGGGDEGDALGSNSSSQPNRVARMPVDRNAPYYNMNHKHRGMAIIFNHEHFDIHSLK  77

Bm      75 SRTGTNVDSDSLSKVLRGLGFSVTVLHNLRAEDINRYIQQISEMDHTDNDCLLVAVLSHG 134
           SRTGTNVDSD+LSKVL+ LGF VTV  NL++E+IN++IQQ +EMDH+D DCLLVAVL+HG
Sf      78 SRTGTNVDSDNLSKVLKTLGFKVTVFPNLKSEEINKFIQQTAEMDHSDADCLLVAVLTHG 137

Bm     135 ELGMLYAKDTHYKPDNLWYYFTADKCPTLAGKPKLFFIQACQGDKLDGGITLSNTETDGS 194
           ELGMLYAKDTHYKPDNLWYYFTADKCPTLAGKPKLFFIQACQGD+LDGGITLS TETDGS
Sf     138 ELGMLYAKDTHYKPDNLWYYFTADKCPTLAGKPKLFFIQACQGDRLDGGITLSRTETDGS 197

Bm     195 SSSSYRIPIHADFLIVFSTVPGYYSWRNTTRGSWFMQSLCEELRNYGTQRDILTLLTFVC 254
            S SYRIP+HADFLI FSTVPGY+SWRNTTRGSWFMQ+LCEELR  GT+RDILTLLTFVC
Sf     198 PSTSYRIPVHADFLIAFSTVPGYFSWRNTTRGSWFMQALCEELRYAGTERDILTLLTFVC 257

Bm     255 QRVALDFESNTPDITPMHQQKQVPCINSMLTRLLLFGKK 293
           Q+VALDFESN PD   MHQQKQVPCI SMLTRLL+FGKK
Sf     258 QKVALDFESNAPDSAMMHQQKQVPCITSMLTRLLVFGKK 296
```

FIG. 3. **A. Predicted amino acid sequence of the *B. mori* caspase-1.** The consensus catalytic site of the caspase is *underlined*. *B*, comparison of *B. mori* and *S. frugiperda* caspase-1 amino acid sequences using the BLAST program. Identical and similar (+) residues are indicated (*middle line*).

formed in the positive ion mode using repetitively full mass spectrometry scan followed by collision-induced dissociation of the most dominant ion selected from the first mass spectrometry scan. The mass spectrometry data were compared with simulated proteolysis and collision-induced dissociation of the proteins in the "nr" data base (NCBI) using Sequest software (J. Eng and J. Yates, University of Washington and Finnigan).

RESULTS

P49 Structure—To learn about the relationship between the structure of P49 structure and its possible function, we performed computer-assisted modeling of P49 based on the recently determined structure of the pancaspase inhibitor P35 (19) (see "Experimental Procedures"). This comparison predicted several domains important for P49-function. (I) P49 domains of high homology to P35 (both polypeptidic chains of 236 and 299 amino acids are depicted in Fig. 1 in *blue* and *green*, respectively) included the following: (*a*) the β-core, composed of a β-barrel domain with a large insertion, which forms the reactive site loop (Fig. 1, *RSL*). The RSL begins at the amphipathic α_1-helix (between Val^{69} and Phe^{83}, Figs. 1 and 7*A*) and traverses the β-sheet central region, exposing the Asp^{94} residue at the apex, in the context of the putative caspase-cleavable motif $^{91}TVTD^{94} \downarrow G$ (which corresponds to the P35 caspase-cleavable motif $^{84}DMQD^{87} \downarrow G$ (19)) and follows downwards rejoining the β-barrel; (*b*) three additional α-helical domains, α_2 (between residues Gly^{115} and Asn^{127}), α_3 (between residues Tyr^{133} and Pro^{146}), and α_4 (between residues Ile^{231} and Arg^{236}) (Fig. 1); (*c*) a side loop (indicated as *loop 3* and *L3* in Fig. 1, *A* and *B*, respectively) between amino acids Leu^{147} and Lys^{167} larger than the correspondent P35 loop (between Lys^{140} and Asp^{147}). (II) The C terminus of P49 (between Lys^{346} and Ile^{446}), homologue to the C terminus of P35 (between Lys^{259} and Ile^{298}), as predicted by secondary structure analysis, is shown in Fig. 1*B* (21). (III) α-Helical regions predicted by secondary structure analysis that are not present in P35 (Fig. 1*B*) are designated $\alpha_{4'}$ (between residues Leu^{237} and Asn^{247}), α_5 (between residues Asn^{279} and His^{298}), and α_6 (between residues Val^{364} and Ile^{383}).

Since P35 was shown as a potent inhibitor of invertebrate and vertebrate caspases, we proceeded to analyze the ability of P49 to inhibit caspase activity.

P49 Function—To study P49 function, we engineered *sl-p49* under the control of the strong baculoviral promoter polyhedrin and isolated the correspondent baculovirus (vAcP49). We overexpressed *sl-p49* protein in insect cells, identified it by protein-sequence analysis that confirmed the putative P49 sequence (21), and used it to produce anti-P49 antiserum (see "Experi-

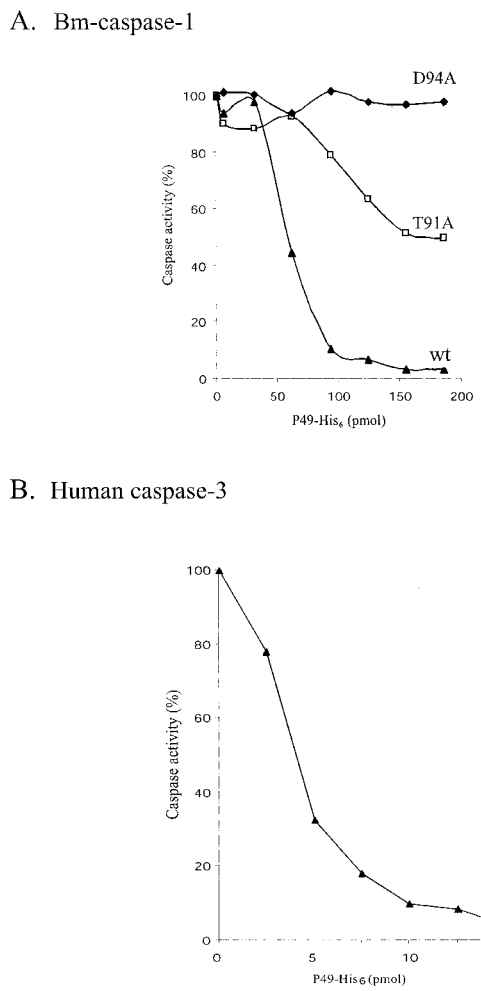

FIG. 4. **Inhibition of insect and human effector caspases by P49.** Increasing amounts of P49H were incubated with *B. mori* caspase-1 (purified by affinity chromatography; see "Experimental Procedures") (*A*) or with human caspase 3 (Cpp32; Biomol, Inc.) (*B*). After 30 min, residual caspase activity was determined colorimetrically at 405 nm using the specific peptidic substrate Ac-DEVD-*p*-nitroanilide.

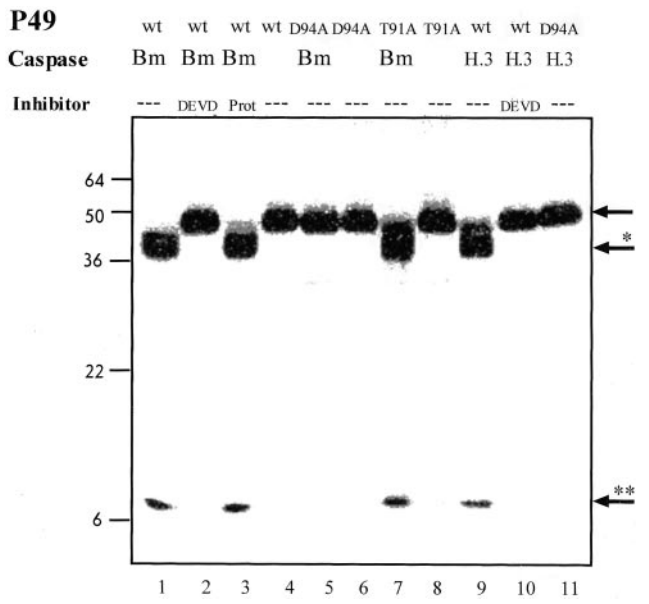

FIG. 5. **D94A is required for P49 cleavage by effector caspases.** ^{35}S-Labeled *in vitro* translated wild type (*wt*) or D94A- or T91A-mutated P49 was incubated for 30 min with *B. mori* caspase-1 (*Bm*) or human caspase-3 (*H.3.*) and then subjected to SDS-PAGE and autoradiography. When indicated, Ac-DEVD-CHO (*DEVD*) or protease (*Prot*) inhibitors were added before the caspase addition. The *arrows* indicate the uncleaved and cleaved (39-kDa (*) and 9.9-kDa (**)) forms of P49. Molecular markers (in kDa) are indicated on the *left*.

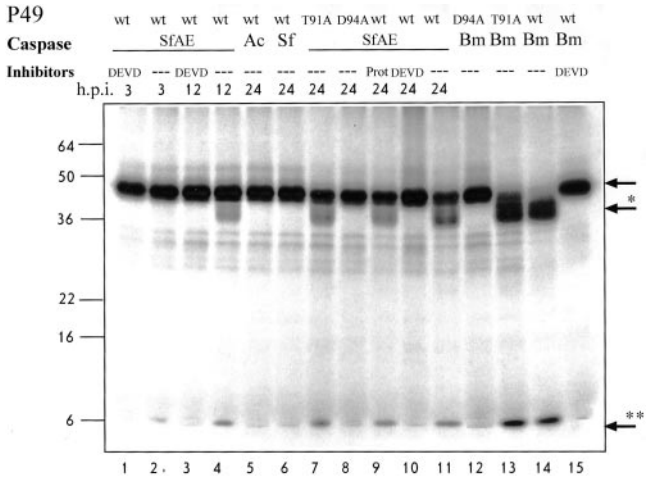

FIG. 6. **Viral induced *S. frugiperda* caspase and *B. mori* caspase-1 cleave P49 to yield similar fragments.** ^{35}S-Labeled *in vitro* translated wild type (*wt*; *lanes 1–6*, *9–11*, *14*, and *15*) or D94A (*lanes 8* and *12*) and T91A (*lanes 7* and *13*) mutated P49 were incubated with SF9 apoptotic (*SfAE*; *lanes 1–4* and *7–11*), mock-infected (*Sf*, *lane 6*), or AcMNPV-infected (*lane 5*) extracts or purified *B. morii* caspase-1 (*Bm*, *lanes 12–15*), and the cleaved polypeptides were resolved in a 15% SDS-polyacrylamide gel followed by autoradiography. The cell extracts were prepared at 3, 12, or 24 h postinfection (*h.p.i.*; *lanes 1* and *2*, *lanes 3* and *4*, and *lanes 5–11*, respectively). When indicated, Ac-DVED-CHO (*DEVD*) or nonspecific protease inhibitors (*Prot*) were added to the reaction mixture (*lanes 1*, *3*, *10*, *15*, and *9*, respectively). The *arrows* indicate the uncleaved and cleaved P49 (*asterisks*). Molecular markers (in kDa) are indicated on the *left*.

mental Procedures"). The antiserum was able to detect P49 synthesis in vAcP49-infected SF9 cells (Fig. 2, *right panel*, *lane vAcP49*). To purify P49, we engineered it with a C-terminal His tag and expressed it using the correspondent recombinant baculovirus vAcP49H (see "Experimental Procedures"). First, we confirmed that the recombinant gene *sl-p49H* indeed expressed a functional protein (P49H) by using a marker rescue assay in which SF9 cells were co-transfected with vAcΔP35/pol+ and a plasmid bearing sl-*p49H* under the control of the *sl-p49* promoter (21). Recovery of the polyhedra-positive virus phenotype due to suppression of apoptosis was indicative of a functional *sl-p49* gene (Table I) (21). P49H was isolated from extracts of vAcP49H-infected SF9 cells (Fig. 2) by affinity chromatography using Ni^{2+}-conjugated agarose beads. The identity of the isolated protein was confirmed by SDS-PAGE electrophoresis followed by immunoblot analysis utilizing anti-P49 antiserum (Fig. 2, *right panel*, *lanes marked P49H*; the full-size P49 molecules are indicated by the *arrow*) and by reacting the vAcP49H-infected cell extract and purified protein with anti-His tag antiserum (Fig. 2, *left panel*, *lanes vAcP49H* and *P49H*, respectively). A smaller polypeptide was detected by the anti-P49 antiserum, but its nature is still under investigation, since it does not bind to the Ni^{2+} column. Also, a higher nonspecific band (over 65 kDa) that reacted with mock-infected and baculovirus-infected extracts was observed consistently (Fig. 2, *right panel*).

P49 Is an Inhibitor of Lepidopteran Caspases—To determine whether P49 is able to inhibit lepidopteran effector caspases, we isolated and expressed caspase-1 of the silkworm *B. mori* (Fig. 3*A*), which is homologue to *S. frugiperda* caspase-1 (Fig. 3*B*), the main lepidopteran caspase responsible for executing the apoptosis program (14, 16) (see below). Incubation of *B. mori* caspase-1

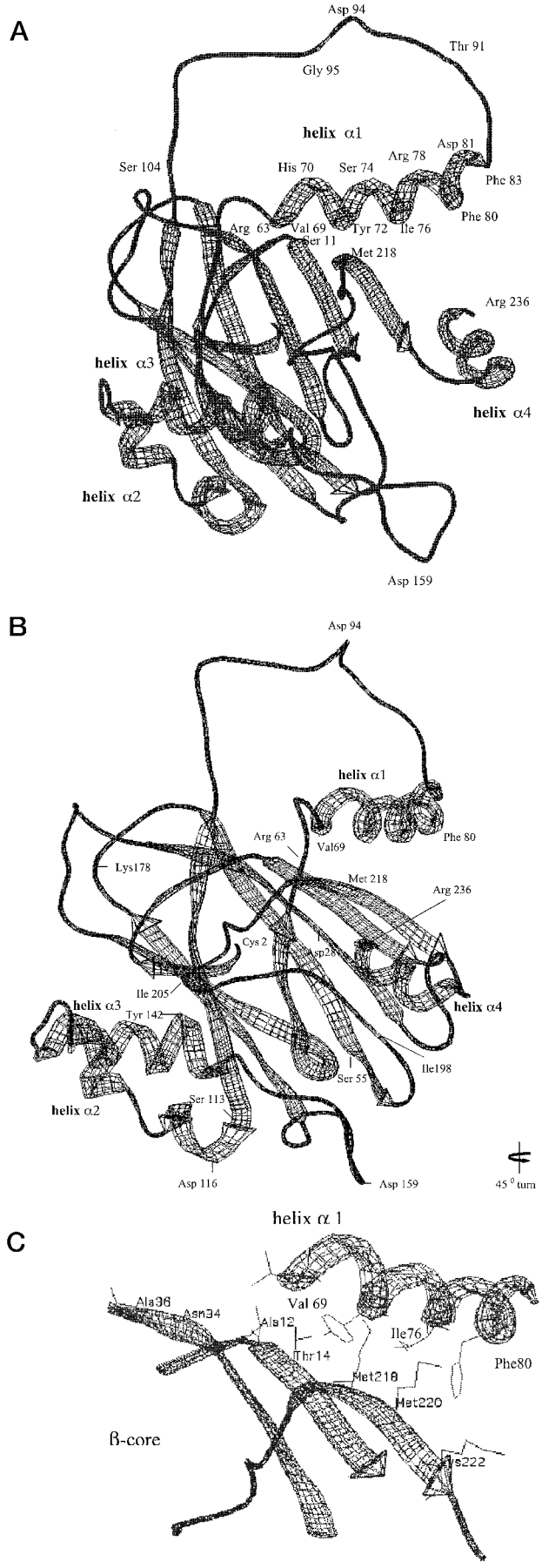

FIG. 7. **Location of mutated amino acid residues in the P49 structure (amino acids 1–236).** *A*, the amino acid residues of the RSL, the amphipathic α_1 helix facing the solvent, and the hydrophobic amino acids facing the β-core are indicated. *B*, 45° rotation of *A*. Residues mutated in the β-core and the α_2, α_3, and α_4 helixes are indicated. *C*, detailed interaction between residues in helix α_1 and the β-core. The *images* were created by using the program Swiss-Model (29, 38) and based on P35 coordinates (Protein Data Bank code 1P35) (20). The specific mutations performed are indicated in Table I.

with increasing amounts of affinity chromatography-purified P49-His_6 resulted in complete inhibition of caspase activity as monitored by the ability of the caspase to cleave the specific substrate DEVD-*p*-nitroanilide (Fig. 4*A*). Our P49 model predicted that amino acid residues at positions P_1–P_4 in the putative caspase recognition motif ^{91}TVTD^{94} could be essential for caspase inhibition by P49. Thus, we mutated Asp^{94} and Thr^{91} residues and analyzed the ability of the mutants to inhibit caspase activity. Indeed, the mutant D94A was unable to inhibit *B. mori* caspase-1, and the mutation T91A affected significantly the ability of P49 to inhibit the caspase (Fig. 4*A*).

To investigate if P49 is able to inhibit a human effector caspase, we performed the same assay using human caspase-3. As can be seen, P49 inhibited the human caspase-3, CPP32, in a dose-dependent manner (Fig. 4*B*). The apparent discrepancy in P49's preference for human caspase-3 over *B. mori* caspase-1 (15 pmol and more than 100 pmol were required to completely inhibit the former and the latter, respectively) was due to different amounts of caspase utilized in each assay (0.3 and 25 pmol for human caspase-3 and *B. mori* caspase-1, respectively).

Asp^{94} Is Required for P49 Cleavage by Caspases—Caspase-inhibition by P35 requires cleavage of the tetrapeptide motif ^{84}DMQD^{87}. Thus we expected that caspase inhibition by P49 would require cleavage of Asp^{94} in the ^{91}TVTD^{94} motif, positioned at the apex of RSL in our model. To test this hypothesis, we incubated *in vitro* translated ^{35}S-labeled P49 with affinity-purified *B. mori* caspase-1. As can be seen, *B. mori* caspase-1 cleaved P49 to yield a large fragment of about 39 kDa and a small fragment of about 9.9 kDa (Fig. 5, *lane 1*, *arrows with asterisks* indicate the cleaved fragments), corresponding to the sizes expected from cleavage at the ^{91}TVTD^{94} motif. P49 cleavage was inhibited when the type II-caspase inhibitor DEVD-CHO (18) was added to the mixture before the addition of P49 (Fig. 5, *lane 2*), but not when a mixture of protease inhibitors that do not inhibit caspases was utilized (Fig. 5, *lane 3*). Moreover, we performed the same experiment utilizing the two mutants in the ^{91}TVTD^{94} motif: D94A and T91A. Incubation of *in vitro* translated P49 mutant proteins with purified *B. mori* caspase-1 showed that the D94A mutation abolished caspase-mediated cleavage of P49, whereas T91A did not abolish it (Fig. 5, *lanes 5* and *7*, respectively). Also, P49 cleavage by human caspase-3 was specific, yielding the 39- and 9.9-kDa fragments, and required aspartate at position 94 (Fig. 5, *lanes 9–11*).

Baculovirus infection activates *S. frugiperda* caspase-1 (16). In order to investigate whether P49 could be cleaved by apoptotic extracts containing *S. frugiperda* caspase-1, *in vitro* translated ^{35}S-labeled P49 was incubated with extracts of SF9 insect cells prepared at various time points after infection with vAcΔP35/pol+ (Fig. 6, *lanes 1–4* and *7–11*, indicated at the *bottom*). It can be seen that P49 was cleaved by apoptotic extracts prepared at 12 and 24 h postinfection to yield the 39- and 9.9-kDa fragments (Fig. 6, *lanes 4* and *9*) identical in size to those obtained by incubation of the protein with *B. mori* caspase-1 (Fig. 6, *lane 14*). Again, P49 cleavage was inhibited by Ac-DEVD-CHO (Fig. 6, *lanes 1*, *3*, *10*, and *15*). No inhibition of P49 cleavage was observed with a mixture of protease inhibitors added to the reaction mixture (Fig. 6, *lane 9*), neither if P49 was incubated with extracts from wild type AcMNPV-infected cells (that synthesize the apoptotic suppressor P35) or

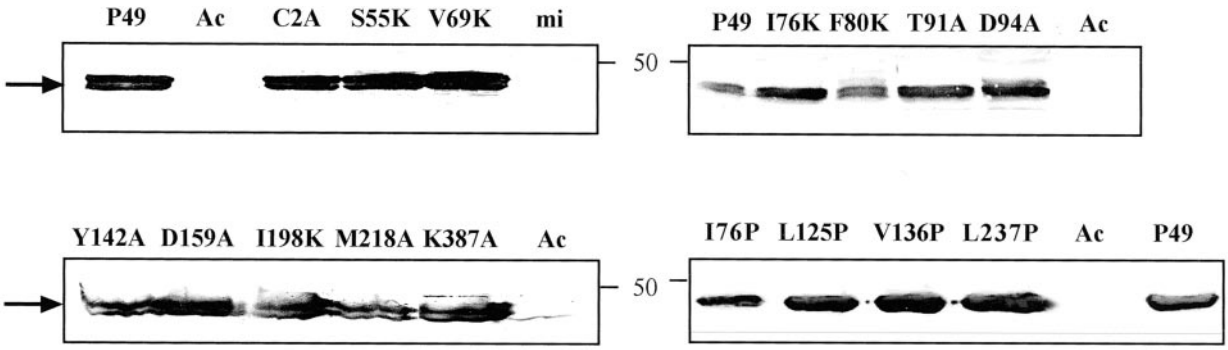

FIG. 8. **Synthesis of wild type and mutated P49 in insect cells.** SF9 cells (10^5) were infected with recombinant baculoviruses expressing wild type or mutant P49 proteins (mutations indicated *above* the *lanes*). At 72 h postinfection, the cell extracts were subjected to SDS-PAGE and immunoblot analysis using anti-P49 antiserum. *Arrow*, P49 size. A molecular marker (kDa) is indicated between the *left* and *right panels*.

from mock-infected SF9 cells (Fig. 6, *lanes 5* and *6*, respectively). Furthermore, the timing of P49 cleavage correlated with the induction of the effector caspase-1 in *S. frugiperda* cells (16) at 12 h after infection with vAcΔP35/pol+ (compare *lanes 2*, *4*, and *7* in Fig. 6). Incubation of T91A and D94A mutants with the apoptotic extracts resulted in cleaved and uncleaved polypeptides, respectively, as obtained by their incubation with purified caspase-3 (Fig. 6, *lanes 7* and *8* and *lanes 13* and *12*, respectively).

Taken together, these results support the idea that the Asp^{94} residue at the consensus caspase cleavage motif ^{91}TVTD^{94} is required for caspase cleavage of P49, to generate the fragments of 39 and 9.9 kDa.

P49 Putative Structure and Inhibition of Apoptosis—We performed a series of site-directed mutations in P49 to test predictions of the model and begin to map P49 domains important for suppression of apoptosis. For that purpose, plasmids bearing wild type or mutated *p49* and vAcΔP35/pol+ were transfected to SF9 cells and examined for their ability to rescue viral replication (polyhedra formation) inhibiting apoptosis. In parallel, we constructed recombinant baculoviruses to establish that indeed the mutant proteins were stably expressed (see below).

First, we targeted the predicted P49 structural elements homologous to P35. Our results are summarized in Table I. The importance of the RSL for the function of P49 was confirmed by utilizing the mutants T91A and D94A in the motif ^{91}TVTD^{94} (Fig. 7*A*). As expected, both mutants were unable to rescue apoptosis (Table I).

We investigated whether residues Val^{69}, Ile^{76}, and Phe^{80}, located at the hydrophobic phase of the helix α_1 motif (Fig. 7, *A* and *C*), interacted with the β-core of the P49 molecule, as has been shown in P35 helix α_1 (20). Thus, disruption of possible hydrophobic interactions by mutagenesis could abolish P49 antiapoptotic function. To test this possibility, three neutral to charged mutations (namely V69K, I76K, and F80K) were inserted separately in P49. Indeed, each of these P49 mutants lost its ability to inhibit apoptosis induced by vAcΔP35/pol+ (Table I). In contrast, substitution of Ile^{76} by the aromatic residue Tyr resulted in a functional protein (Table I). Moreover, mutation R63Q of a residue predicted to be at a turn preceding helix α_1 (Fig. 7*A*) did not affect the ability of P49 to rescue viral replication (Table I). Mutation of Met^{218} (M218A), located in a β-sheet of the β-core motif (Fig. 7, *A* and *C*) predicted to interact with helix α_1, resulted in nonfunctional P49 (Table I).

Mutations that could distort the stability of the β-barrel motif were predicted to result in loss-of-function P49. Thus, charged-to-neutral (Ala) and neutral-to-charged mutations D28A and S55K, respectively, in putative β-sheets of the β-core motif (Fig. 7*B*) yielded nonfunctional P49, in contrast to the alanine replacement mutations C2A and S113A (Table I). Mutations D159A, K178A, I205K, and K387A of residues predicted to be located in loops of the β-core motif or facing the solvent (see Fig. 7*B*; data not shown) did not affect the ability of P49 to suppress apoptosis (Table I). Interestingly, the neutral-to-charged mutation I198K placed in a loop (probably in the β-core) resulted in nonfunctional P49. Mutation at Y142A in helix α_3 yielded nonfunctional P49 (Fig. 7*B* and Table I).

The contribution of P49's putative α-helical regions α_1, α_2, α_3, $\alpha_{4'}$, and α_6 of P49 to inhibit apoptosis was analyzed by introducing proline residues (known to disrupt α-helical regions) to obtain the corresponding mutants I76P, L125P, V136P, L237P, and L376P. Mutants I76P, L125P, and L237P lost their ability to inhibit apoptosis (Table I).

Insertion of six His residues (His_6 tag) at the N terminus, located at the center of the β-barrel, resulted in a nonfunctional P49 in contrast to C-terminal insertion.

All of the mutant proteins were synthesized to comparable levels in insect cells (shown in Fig. 8 for the proteins that lost their ability to inhibit apoptosis described in Table I; positive mutants C2A, V136P, D159A, and K387A were also included).

Taken together, the mutagenesis results support our model of P49. Moreover, they indicate that at least the α-helical regions α_1, α_2, and $\alpha_{4'}$ are required for P49's antiapoptotic function.

DISCUSSION

In this study, we expressed and analyzed the product of the *sl-p49* gene of the *S. littoralis* nucleopolyhedrovirus. We found, as predicted by the nucleotide sequence (21), that *sl-p49* coded for a protein of about 49 kDa. The putative P49 amino acid sequence was confirmed by amino acid sequencing, and we built a model of P49, based on its homology to the caspase inhibitor P35 from the *A. californica* nucleopolyhedrovirus, whose crystal structure was recently resolved (19). Our three-dimensional model of P49 included the N-terminal 236 amino acid residues. Also, we made some predictions based on the analysis of the secondary structure of P49 and applied them to study some features of the C-terminal part of the molecule (amino acid residues 239–446). Thus, we identified the following: a β-core, three additional alpha helical domains, and a side loop.

β-Core—The β-core was composed of a β-barrel domain with a large insertion that forms the RSL. The RSL begins at an amphipathic α_1 helix (between Val^{69} and Phe^{83}) (Figs. 1 and 7*A*) and traverses the β-sheet central region, exposing the Asp^{94} residue at the apex, in the context of the putative caspase-cleavable motif ^{91}TVTD^{94} ↓ G, and follows downwards, rejoining the β-barrel. We determined that indeed the amino acid residues Thr^{91} and Asp^{94} were required for P49 antiapoptotic function (Table I), Asp^{94} for caspase cleavage (Fig. 5), and Thr^{91} and Asp^{94} for efficient caspase inhibition (Fig. 4). The amino acid residues of the helix α_1 domain, which face the

β-core, appear to interact with the adjacent amino acid residues from the β-sheet and are required for the antiapoptotic function of P49. Thus, replacement of hydrophobic residues Val^{69}, Ile^{76}, and Phe^{80} by charged residues abolished the ability of P49 to rescue apoptosis (Table I), in contrast to their replacement by hydrophobic residues (*e.g.* I76Y). These results are in accordance with the role proposed for P35 helix α_1 in maintaining the structure of the RSL (19, 20). Moreover, whereas cleavage of Asp^{87} of the caspase recognition motif ^{84}DQMD^{87} of P35 was required for its antiapoptotic activity, it was not sufficient for stable association and inhibition of caspases (19, 20). Resolution of the crystal structure of a mutant in P35-α_1 helix (V71P) suggested that it might be required to enable conformational changes after cleavage required for the formation of a stable complex between P35 and the caspase (20, 31, 32). A similar role may be attributed to P49-α_1 helix, and further studies will be required to show P49-caspase association and the contribution of the α_1 helix to the mechanism of apoptosis inhibition by P49.

The Thr residue at position P_4 of the caspase cleavage consensus motif is important to proper inhibition by caspases belonging to group II (18). The T91A mutation changed that specificity; thus, we expected that caspase inhibition by this mutant should be less effective. Indeed, caspase inhibition studies that we performed with the T91A-purified P49 and *B. mori* caspase-1 validated that hypothesis (Fig. 4). A possible explanation for the behavior of this mutant is that although cleavage by caspase occurs, the P49 mutant molecule does not remain bound to the caspase, and it dissociates from it, failing to inhibit it irreversibly (16).

Additional α-Helical Domains—Three additional α-helical domains, α_2 (between residues Gly^{115} and Asn^{127}), α_3 (between residues Tyr^{133} and Pro^{146}), and α_4 (between residues Ile^{231} and Arg^{236}) (Figs. 1 and 7*A*) homologous to those present in the P35 structure (Fig. 1) (19) and α-helical regions (predicted by secondary structure analysis, that are not present in P35) were designated $\alpha_{4'}$ (between residues Leu^{237} and Asn^{247}), α_5 (between residues Asn^{279} and His^{298}), and α_6 (between residues Val^{363} and Ile^{385}). Our mutagenesis data suggest that helical regions α_1, α_2, and $\alpha_{4'}$ are required for P49 function (Table I).

Side Loop—A side loop (indicated as *loop 3* and *L3* in Fig. 1, *A* and *B*, respectively) between amino acids Leu^{147} and Lys^{167} was larger than the correspondent P35 loop (between Lys^{140} and Asp^{147}). Replacement of Asp^{159} by Ala did not affect P49 function (Table I).

Also, our model suggested that the P49 N terminus would be embedded in the β-core and would be disturbed by introduction of the six His residues of the His tag. Indeed, this mutated P49 was not functional. Introduction of the six His residues of the His tag at the C terminus did not affect P49 function, suggesting that the C terminus of the protein could be facing the solvent.

Overall, analysis of the modeled P49 structure revealed a pretty good correlation between mutational disruption of defined secondary structures (α-helical regions and β-sheets) (Fig. 7, *A* and *B*) and loss of P49 function (Table I). Mutations in intervening loops, predicted not to disrupt the secondary structure, did not abolish P49's antiapoptotic function (Table I).

P49 was able to inhibit the insect effector *B. mori* caspase-1 and *S. frugiperda* caspase activities as well as the human effector caspase-3 (Fig. 4) and was cleaved by caspases to yield 39- and 9.9-kDa fragments (Figs. 5 and 6). Despite the fact that the caspase cleavage motif in P49 is ^{91}TVTD^{94} and that in P35 is ^{84}DQMD^{87}, both inhibit human caspase-3. This suggests that if P49 has a different (broader) selectivity for caspases than P35, other structural elements present in P49 and absent in P35 could confer it. In this respect, it is noteworthy that the α-helical regions of P49 α_1, α_2, and $\alpha_{4'}$ were required for its antiapoptotic function. In contrast, helix α_2 was not required for P35 suppression of apoptosis (20).

The high structural homology of P49 and P35 suggests that these molecules bear a scaffold common to baculovirus apoptotic suppressor proteins that could be designated a P35-like family of proteins. Indeed, P35-like proteins were identified in the genomes of the baculoviruses BmNPV (33), CuniNPV (34), LsNPV (35), TnMNPV (36), and SlpltMNPV (37). It will be interesting to search for the presence of more homologous proteins in the animal kingdom and more specifically in the genomes of arthropods, the natural hosts of baculoviruses. Moreover, our results indicate that P49 may serve as a novel tool to analyze the contribution of different components of the caspase chain participating in the apoptotic response in organisms not related phylogenetically.

REFERENCES

1. Jacobson, M. D., Weill, M., and Raff, M. C. (1997) *Cell* **88,** 347–354
2. Steller, H. (1995) *Science* **267,** 1445–1449
3. Clem, R. (2001) *Cell Death Differ.* **8,** 137–143
4. Chang, H. Y., and Yang, X. (2000) *Microbiol. Mol. Biol. Rev.* **64,** 821–846
5. Teodoro, J. G., and Branton, P. (1997) *J. Virol.* **71,** 1739–1746
6. Miller, L. K., Kaiser, W. J., and Sehsagiri, S. (1998) *Semin. Virology* **8,** 445–452
7. Birnbaum, M. J., Clem, R. J., and Miller, L. K. (1994) *J. Virol.* **68,** 2521–2528
8. Crook, N. E., Clem, R. J., and Miller, L. K. (1993) *J. Virol.* **67,** 2168–2174
9. Clem, R. J., and Miller, L. K. (1994) *Mol. Cell. Biol.* **14,** 5212–5222
10. Liston, P., Roy, N., Tamai, K., Lefebvre, C., Baird, S., Chertonhorvat, G., Farahani, R., Mclean, M., Ikeda, J. E., Mackenzie, A., and Korneluk, R. G., (1996) *Nature* **379,** 349–353
11. Duckett, C. S., Nava, V. E., Gedrich, R. W., Clem, R. J., Vandongen, J. L., Gilfillan, M. C., Shiels, H., Hardwick, J. M., and Thompson, C. B. (1996) *EMBO J.* **15,** 2685–2694
12. Hay, B. A., Wassarman, D. A., and Rubin, G. M. (1995) *Cell* **83,** 1253–1262
13. Xue, D., and Horvitz, H. R. (1995) *Nature* **377,** 248–251
14. Ahmad, M., Srinivasula, S. M., Wang, L., Litwack, G., Fernandes-Alnemri, T., and Almemri. E. S. (1997). *J. Biol. Chem.* **272,** 1421–1424
15. Bump, N. J., Hackett, M., Hugunin, M., Seshagiri, S., Brady, K., Chen, P., Ferenz, C., Franklin, S., Ghayur, T., Li, P., Licari, P., Mankovich, J., Shi, L. F., Greenberg, A. H., Miller, L. K., and Wong, W. W. (1995) *Science* **269,** 1885–1888
16. Bertin, J., Mendrysa, S. M., Lacount, D. J., Gaur, S., Krebs, J. F., Armstrong, R. C., Tomaselli, K. J., and Friesen, P. D. (1996) *J. Virol.* **70,** 6251–6259
17. Zhou, Q., Krebs, J. F. Jnipas, S. J., Price, A., Alnemri, E. S., Tomaselli, K. J., and Salvensen, G. S. (1998) *Biochemistry* **37,** 10757–10765
18. Thornberry, N. A., and Labeznik, Y. (1998) *Science* **281,** 1312–1316
19. Fisher, A. J., Cruz, W., Zoog, S. J., Schneider, Ch. L., and Friesen, P. D. (1999) *EMBO J.* **18,** 2031–2039
20. Zoog, S. J., Bertin, J., and P. D. Friesen (1999) *J. Biol. Chem.* **274,** 25995–26002
21. Du, Q., Lehavi, D., Faktor, O., Qi, Y., and Chejanovsky, N. (1999). *J. Virol.* **73,** 1278–1285
22. Hink, W. F. (1970) *Nature* (*Lond.*) **225,** 466–467
23. Summers, M. D., and Smith, G. E. (1978) *Tex. Agric. Exp. Stn. Bull.* **1555**
24. Cartier, J. L, Hershberger, P. A., and Friesen, P. D. (1994) *J. Virol.*, **68,** 7728–7737
25. Stennicke, H. R., and Salvesen, G. S. (1999) *Methods Companion Methods Enzymol.* **17,** 313–319
26. Chejanovsky, N., and Gershburg, E. (1995) *Virology* **209,** 519–525
27. Gershburg, E., Rivkin, H., and Chejanovsky, N. (1997) *J. Virol.* **71,** 7593–7599
28. Kelley, L. A, MacCallum, R. M., and Sternberg, M. J. E. (2000) *J. Mol. Biol.* **299,** 501–522
29. Guex, N., and Peitsch, M. C. (1997) *Electrophoresis* **18,** 2714–2723
30. Papworth, C., Bauer, J. C., and J., Braman (1996) *Strategies* **9,** 3–4
31. de la Cruz, W., Friesen, P. D., and Fisher, A. J. (2001) *J. Biol. Chem.* **276,** 32933–32939
32. Xu, G., Cirilli, M., Huang, Y., Rich, R. L., Myszka, D., and Wu, H. (2001) *Nature* **410,** 494–497
33. Kamita, S. G., Majima, K., and Maeda, S. (1993) *J. Virol.* **64,** 455–463
34. Afonso, C. L., Tulman, E. R., Lu, Z., Balinsky, C. A., Moser, B. A., Becnel, J. J., Rock, D. L., Kutish, G. F. (2001) *J. Virol.* **75,** 11157–11165
35. Qi, Y., Liu, Q., Peng, Y., Li, L., Pei, Z., Liu, Y. (2001) *Arch. Virol.* **146,** 2149–2163
36. Dai, X., Shi, X., Pang, Y., Su, D. (1999) *J. Gen Virol.* **80,** 1841–1845
37. Pang, Y., Yu, J., Wang, L., Hu, X., Bao, W., Li, G., Chen, C., Han, H., Hu, S., Yang, H. (2001) *Virology* **287,** 391–404
38. Peistch, M. C. (1995) *Bio/Technology* **13,** 658–660